Journal of Nuclear Materials 393 (2009) 473–480

Contents lists available at ScienceDirect

Journal of Nuclear Materials

journal homepage: www.elsevier.com/locate/jnucmat

Optical properties of Al mirrors under impact of deuterium plasma ions in experiments simulating ITER conditions

A.F. Bardamid [b], A.I. Belyaeva [c], J.W. Davis [d,*], M.V. Dobrotvorskaya [e], A.A. Galuza [c], L.M. Kapitonchuk [f], V.G. Konovalov [a], I.V. Ryzhkov [a], A.F. Shtan' [a], K.A. Slatin [c], S.I. Solodovchenko [a], V.S. Voitsenya [a]

[a] IPP NSC KIPT, 61108 Kharkov, Ukraine
[b] Taras Shevchenko National University, 01033 Kiev, Ukraine
[c] National Technical University "KhPI", 61002 Kharkov, Ukraine
[d] University of Toronto Institute for Aerospace Studies, 4925 Dufferin St., Toronto, ON, Canada M3H5T6
[e] NSC Single Crystal Institute, Kharkov, Ukraine
[f] E.O.Paton Electric Welding Institute, Kiev, Ukraine

ARTICLE INFO

Article history:
Received 1 June 2009
Accepted 4 July 2009

ABSTRACT

The ion-induced modification of aluminum alloy mirrors, under bombardment by deuterium plasma ions has been investigated as a simulation of the environment effects on in-vessel mirrors in ITER. Ellipsometry and reflectrometry have been used to characterize the mirror surface, along with several surface diagnostic techniques (XPS, Auger, SIMS). The results of multiangular- and spectro-ellipsometry were analyzed using both a bare surface model, and effective medium model; the medium was composed of Al, Al_2O_3 ($Al(OD)_3$ or AlOOD), and voids. It was found that the reflectance decreases following exposure to keV-range ions, but can be restored by subsequent exposing the mirror to low-energy ions (~60 eV). Chemical processes related to an increased oxide layer are thought to be responsible for the decrease in reflectance, while the reduction of the oxide layer following low-energy D^+ exposure may lead to the return of high reflectance. By comparing the measurements with the results of modeling, a mechanism is suggested to explain the experimental data. The mechanism is based on: (1) chemical processes in a surface layer and (2) changes in the thickness and roughness of the surface layer.

© 2009 Elsevier B.V. All rights reserved.

1. Introduction

Aluminum is one of very few metals with a high reflectance (~90%) which is only weakly dependent on wavelength (starting from ~200 nm) [1]; a property which makes it attractive for diagnostic mirrors in fusion experiments such as ITER. However, aluminum has not been considered a viable material for in-vessel mirrors for ITER due to the rapid degradation of reflectance, R, under deuterium ion bombardment [2,3]. This is in comparison with other materials investigated under similar conditions: exposure to a deuterium plasma with a wide energy distribution (0.1–1.0 keV), measuring reflectance in the range λ = 250–650 nm.

Fig. 1a shows the reflectance of Al mirrors at three wavelengths as a function of the ion-sputtered layer thickness, $R(h)$ (h was found by weight loss measurements) [2]. A comparison with other metals at λ = 600 nm is shown in Fig. 1b. The latter graph clearly demonstrates that the drop in $R(h)$ is much faster for Al than for other metals, including copper, despite the fact that the sputtering yield for copper is higher than that for Al [4]. This comparatively rapid degradation has led to little consideration of Al for first mirrors in ITER, where sputtering by charge-exchange atoms is expected to play one of the major roles in then degradation of mirror optical properties.

We have returned to the study of Al mirrors, following our work with Be mirrors [5,6] where it was determined that ion-induced chemical processes in an oxidized surface layer played an important role in the alteration of optical characteristics. It is well known (e.g., [7]) that a diagonal analogy for aluminum and beryllium in the periodic table is stronger than between many other pairs of elements. As will be shown below, a high degree of similarity also exists in the behavior of mirrors of these metals when they are exposed to deuterium plasma ions.

Our new experiments with Al mirrors indicate that ion-induced chemical processes can modify the composition and thickness of a near-surface layer, with direct impact on optical properties. The analysis of these results, and comparisons with published data suggest that these chemical processes are typical for cases of deuterium ion-impact under high-vacuum conditions.

A noticeable deterioration of Al mirror optical properties under γ-irradiation in a humid atmosphere at room temperature and at 250 °C was linked to the accumulation of hydroxide $Al(OD)_3$ and the compound AlOOD on the mirror surface [8]. The production of similar compounds also took place when an Al-oxide film was

* Corresponding author.
E-mail address: jwdavis@starfire.utias.utoronto.ca (J.W. Davis).

0022-3115/$ - see front matter © 2009 Elsevier B.V. All rights reserved.
doi:10.1016/j.jnucmat.2009.07.003

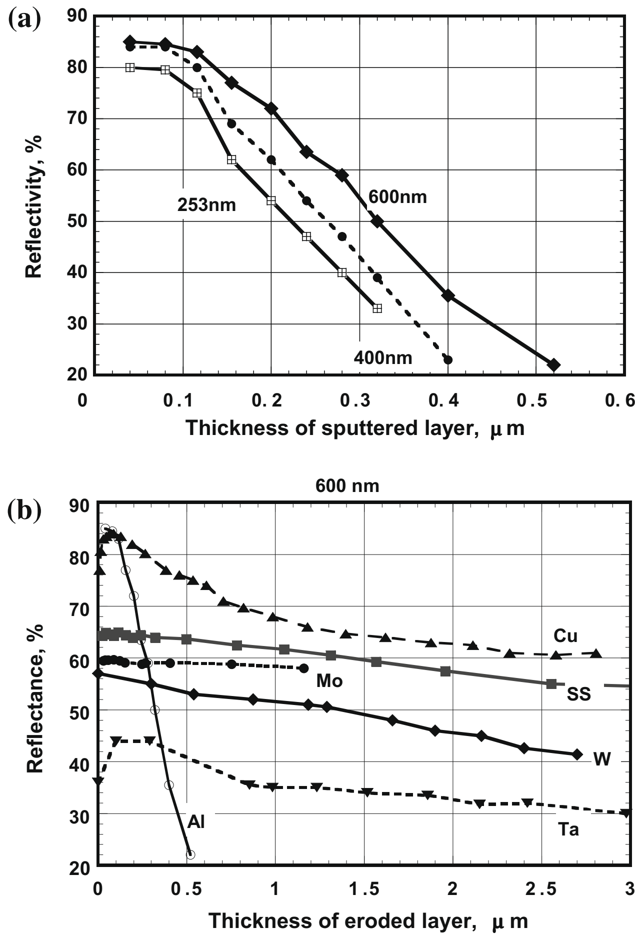

Fig. 1. Dependence of reflectance on thickness of layer sputtered due to ion bombardment: (a) for Al mirrors at three wavelengths (from Ref. [2]); (b) for several metals at $\lambda = 600$ nm (from Ref. [3]).

deposited under high-vacuum conditions with background traces of water vapor [9,10]. The spread of data on optical (references in [9]) and elastic (references in [10]) properties of Al_2O_3 films observed for similar high-vacuum deposition experiments is connected to some uncontrolled level of hydroxides, as stated by the authors of the papers [9,10].

The objective of the present paper is to analyze the mechanism responsible for the rapid degradation of optical properties of Al mirrors. In doing so, we hope to rehabilitate aluminum as a perspective material for in-vessel mirrors in fusion devices.

2. Experimental

The mirror specimens, disks 22 mm in diameter and 3 mm thick, were fabricated of aluminum alloy (duraluminium®) with small impurity concentrations of Cu, Mg and Mn (below we will call these samples as Al samples). Plasma ions were produced in a double-mirror magnetic configuration operated at the electron cyclotron resonance (magnetron frequency 2.37 GHz) [11,12]. The base pressure in the vacuum system was $\sim 2 \times 10^{-4}$ Pa, while during operation the deuterium pressure was $\sim 2 \times 10^{-2}$ Pa. At a magnetron power of $\sim$400 W, the plasma parameters were: $n_e \sim 10^{16}$ m^{-3}, $T_e \leqslant 5$ eV. The water-cooled specimen holder was placed on the system axis, a little outside the magnetic mirror, and was biased negatively at a fixed potential in the range 50–1500 V, or with a variable voltage to provide a wide range ion-energy distribution.

The reflectance was measured *ex situ* after every exposure to ion bombardment. A two-channel scheme [13] was used for studying the spectral dependence of the reflectance at normal incidence, $R(\lambda)$, over the range $\lambda = 220$–650 nm. In this scheme the focused image of the monochromator output slit falls on the mirror under the test. The solid angle of the cone of the luminous flux that falls on the photomultiplier after reflection from the mirror is $\sim 1.2 \times 10^{-2}$; thus, primarily the specular component of the reflected light was measured. Mass changes of the mirror samples were also measured after each bombardment, with an accuracy of 20 μg.

2.1. Ellipsometry

Spectral reflectance was also evaluated by spectral ellipsometry ($\lambda = 350$–750 nm) with a rotating analyzer (RAE scheme) using a bare surface model. The measurements were made at a near-pseudo-Brewster incidence angle 72°, leading to high sensitivity to surface optical properties. The values for the optical indices (refraction and extinction) were obtained by the multiangular method (MAI) using a laser null-ellipsometer (LEF-3M-1, $\lambda = 632.8$ nm). The data were processed using a model consisting of a homogeneous single layer film (*f*) on an Al substrate (*s*) using the effective medium model.

The error in the angle of incidence was $\sim 0.01°$ for the both ellipsometers; errors in the ellipsometric angles were $\delta\Delta \leqslant \pm 0.04°$, $\delta\Psi \leqslant \pm 0.02°$ for the null-ellipsometer and $\delta\Delta \leqslant \pm 0.05°$, $\delta\Psi \leqslant \pm 0.03°$ for the RAE. As is customary in ellipsometry, the Ψ parameter is defined as the change of the ratio of amplitudes of light waves (parallel, p-component and perpendicular, s-component) and Δ is defined as the difference between phase shifts of the parallel and perpendicular components of the light. The measured ellipsometric parameters Ψ and Δ are related to the surface dielectric functions by means of the fundamental ellipsometric equation [14]:

$$\tan \Psi e^{i\Delta} = \frac{R_p}{R_s}, \tag{1}$$

where R_p and R_s are the complex Fresnel reflection coefficients for the parallel (p) and perpendicular (s) components of the light, respectively.

The major task in ellipsometry consists in finding optical parameters for the film-substrate system from the experimental values of Ψ and Δ. In order to solve this task, an adequate model of the surface is required (i.e., to set an explicit form of R_p and R_s), which is then used in Eq. (1).

Several models for the analysis of the ellipsometric data were tried. To first approximation, the surface can be considered to be a bare surface. To refine this model one can assume a bare surface consisting of Al metal which is microscopically rough. This means that there is an effective medium consisting of voids (absence of any material) and Al metal. Using the BEMA (Bruggeman Effective Media Approximation) the effective complex refractive index $N = n - ik$ of the effective medium can be found from [14]:

$$\sum_j f_j \frac{N_j^2 - N^2}{N_j^2 + 2N^2} = 0, \quad \sum_j f_j = 1, \tag{2}$$

where f_j is the volume fraction of the jth component.

The choice of a physically reasonable model is an intricate problem which requires the incorporation of additional information. Minimization of the squared error σ:

$$\sigma = \frac{1}{M}\left(\sum_{i=1}^{M}\left[\left(\Psi_i^{\exp} - \Psi_i^{calc}\right)^2 + \left(\Delta_i^{\exp} - \Delta_i^{calc}\right)^2\right]\right)^{\frac{1}{2}} \tag{3}$$

may be used to determine the model which best approximates the experimental data. In (3) $\Psi_i^{\exp}$ and $\Delta_i^{\exp}$ are the experimental values of ellipsometric parameters and Ψ_i^{calc} and Δ_i^{calc} are the calculated

ones. M is the number of measurements made at different conditions, i.e., incidence angle, wave length, immersion liquid etc.

The minimum value of σ may serve as a measure of the quality of the surface model when several surface models are being compared. On the other hand, even a high-quality approximation (low σ) does not guarantee the correctness of the model. Thus, substantiation of the model must be done very thoroughly [14].

The apparent reflectance at normal incidence, R, as calculated from the ellipsometric parameters is a good measure of the real normal-incidence reflectance. In general R is less sensitive to changes in the surface properties than the apparent complex index of refraction, which is less sensitive than the ellipsometrically determined parameters Ψ and Δ.

2.2. XPS analysis

The uppermost surface layer composition of the Al samples was analyzed by X-ray photoelectron spectroscopy (XPS) using a XPS-800 Kratos spectrometer. The pressure in the vacuum chamber was $\sim 10^{-6}$ Pa; photoelectrons were excited by MgK_{α} radiation ($h_{\gamma} = 1253.6$ eV); the X-ray tube power was 15 kV × 20 mA. The electron energy resolution was 1 eV, the accuracy of measuring the binding energy ~0.3 eV. For layer-by-layer etching of the sample, an argon ion beam was used with energy 1–2 keV ($j = 8 \times 10^{-2}$ A/m^2). For quantitative analysis of the surface layer composition a comparison of areas under the lines Be1s, C1s, O2s, Al2p, Ar2p of the core levels was made, taking into account the sensitivity coefficients.

2.3. Auger and SIMS analysis

The depth distribution of near-surface layer composition was investigated by means of Auger (AES) and secondary ion mass spectrometry (SIMS) using the combined installation LAS 2000 (Riber). For layer-by-layer analysis when providing these measurements, an argon ion sputter beam was used with energy $E_{Ar+} = 4$ keV in the AES case and $E_{Ar+} = 5$ keV in the SIMS case. The background pressure during measurements was $\sim 5 \times 10^{-8}$ Pa, the sputtering rate ~11 nm/min and ~1 nm/min, respectively. No additional cleaning procedures were applied prior to AES and SIMS measurements following specimen exposure in the DSM-2 stand.

Specially prepared specimens of smaller size (7 × 7 mm^2) were used for the Auger and SIMS analysis, which, however, were not polished to a high mirror quality.

2.3.1. Auger analysis

The analysis spot size was ~10 μm, and the identification of elements and AlO was carried out by using the etalon reference table.

2.3.2. SIMS analysis

A distinct advantage of the SIMS technique over the abovementioned methods is that SIMS analysis allows for the detection of hydrogen in the spectrum. To avoid the edge effects in an ion beam etching crater, special methodical precautions were undertaken: the measurement area was 1 × 1 mm^2 while the sputter-crater size was 2 × 2 mm^2. Both, positive and negative secondary ions of atoms, molecules and molecular fragments of compounds on the surface were registered up to 100th atomic mass. For quantitative comparison of mass-spectra of different samples, the normalization was provided using $^{27}Al^{+}$ signal of one of samples.

3. Experimental results

Prior to any measurements, the specimen surfaces were first cleaned with low-energy (60 eV) D^{+} ions (stage 0). This was done to remove the organic residue remaining on the surface following the rinsing of samples in acetone after polishing. Figs. 2a and b show the angular dependence of the ellipsometric parameters Ψ and Δ as obtained by laser ellipsometry for the initial (cleaned) surface, and after three ion bombardment stages. There were two bombardment steps with 1.35 keV ions to a fluence of 1.5×10^{23} ions/m^2 (stage 1) and 2.5×10^{23} ions/m^2 (stage 2) respectively. As a result of the ion bombardment, a decrease in the values of Ψ and Δ occurred, dependent on the angle of incidence, with the greatest decreases occurring at large angles. Fig. 2c shows the dependence of these parameters as a function of ion fluence for the most sensitive angle, $\theta = 72.5°$. As indicated

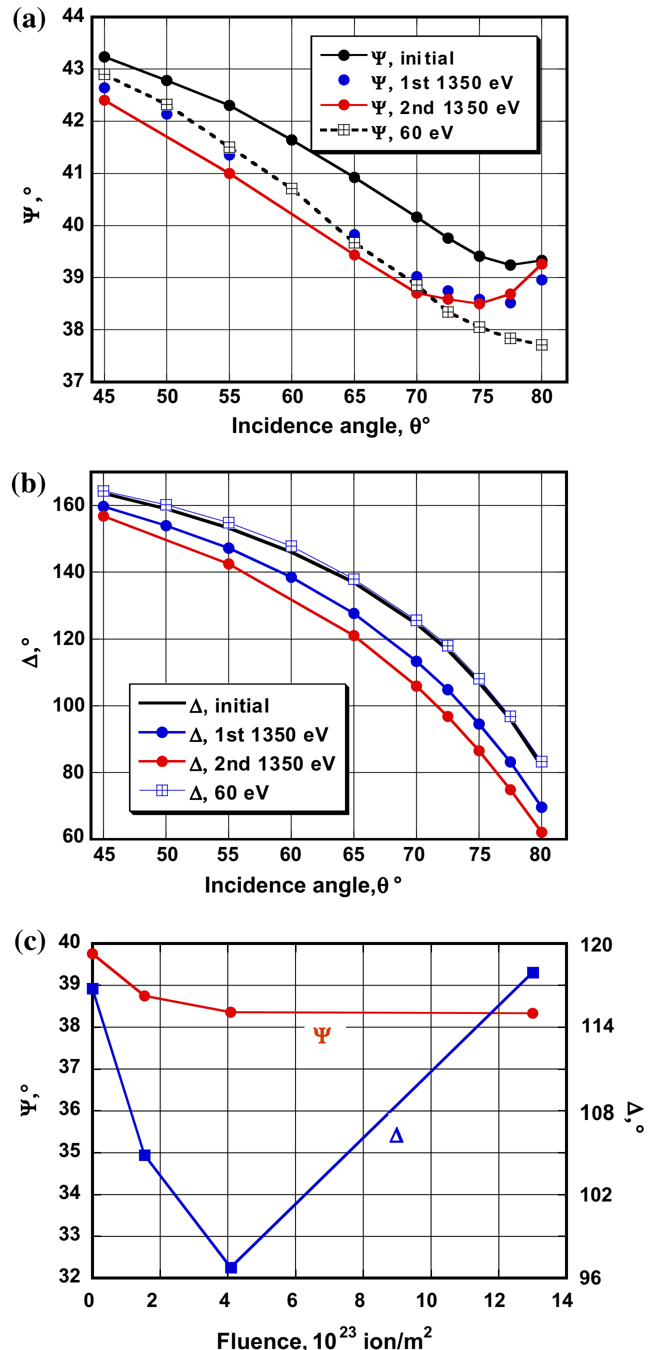

Fig. 2. Angular dependences of ellipsometric parameters Ψ (a) and Δ (b) at various ion fluences ($\lambda = 633$ nm); (c) dependence of ellipsometric parameters at incidence angle 72.5° on ion fluences ($\lambda = 633$ nm).

Table 1
Optical constants (n_f, k_f), thickness (d_f) and reflectivity (R) of the film (f) on Al substrate (s) after laser ellipsometry (λ = 632.8 nm). σ is the approximation quality (3).

Stage	Conditions of measurements	n_f	k_f	d_f (nm)	R	σ
0	Initial	1.6	0	3	84.3	0.031
1	After 1st 1350 eV	1.57	0.25	11	81.9	0.039
2	After 2nd 1350 eV	1.49	0.2	19	79.7	0.029
3	After 60 eV	1.15	0.35	3	84.2	0.14

in the figure, at this angle Ψ decreases monotonically, while Δ returns to its initial value following a long exposure to the low-energy ions (stage 3).

Table 1 presents the optical constants calculated using the MAI method based on the experimental results from Figs. 2a and b. A model of the homogeneous film (f) on an Al substrate (s) is assumed. These values are necessarily approximations since the optical constants for the Al substrates were unknown; values of $n_s = 1.2$ and $k_s = 5.12$ were used. The approximated values were obtained by modeling the initial state of the Al specimen as a homogeneous film of Al_2O_3 ($d_f \geqslant 3$ nm [7]) with unknown optical constants on a metal substrate. The refractive index n_f decreases, while the extinction coefficient (k_f) increases with sequential ion irradiations. However, the film thickness d_f and the reflection coefficient R return to the initial value following stage 3, corresponding to the low-energy ion bombardment, although the extinction coefficient (k_f) continues to stay at a non-zero level.

It should be emphasized that for stages 0–2 the fitting error σ (Table 1 last column) is similar to the experimental accuracy, but it increases by a factor of 5 following stage 3. This implies that the single layer homogeneous film model is no longer adequate and that a more complex interpretation of the surface processes is required.

Fig. 3 shows the spectral reflectance of the Al mirror at each of the four stages of the experiment. Solid symbols represent the ellipsometry data (RAE), while open symbols indicate results for the direct measurements of reflectance at normal incidence. It is evident that bombardment with 1.35 keV ions results in a decrease of reflectance which is more pronounced at shorter wavelengths. Subsequent exposure of the surface to low-energy ions results in almost full restoration of $R(\lambda)$. While the ellipsometry and direct reflectance measurements are qualitatively similar, there are noticeable quantitative differences following the 1.35 keV ion exposure.

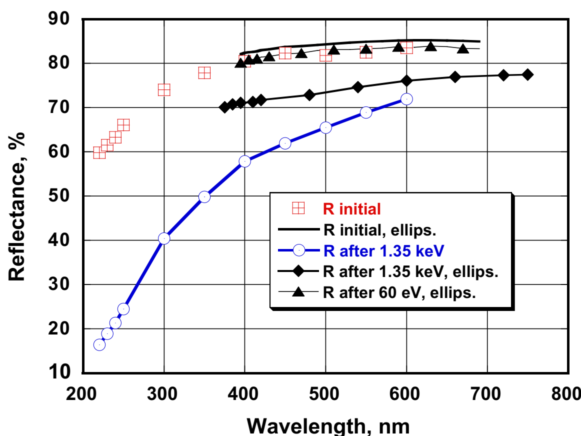

Fig. 3. Spectral dependences of reflectance for Al mirror sample: initial and after successive bombardment with ions of 1350 and 60 eV; full symbols correspond to calculations using the ellipsometric data (RAE) and open symbols are results of direct measurements of reflectance at normal incidence.

The 'drop-restoration' cycle was repeated several times on one specimen; the reflectance measured at two wavelengths is shown as a function of total fluence in Fig. 4. For the 'drop' phases marked 1, 2 and 4 on the figure, the decrease in reflectance was due to ions with fixed energy (E_i = 1.35 keV). In the case marked as 3, the decrease was due to bombardment with the ion energy distributed in the range 0.1 < E_i < 1.5 keV. This latter case is almost an exact repeat of our previous experiments [2,3], where the ion energy was distributed in the range 0.1 < E_i < 1.0 keV, the major difference being a several-times smaller ion fluence in the present case. Thus we believe that the ion-induced degradation of Al mirror optical properties observed previously [2,3] would have been reversible as in the current experiments, and was not connected with the development of surface roughness.

It is observed from Fig. 4, that an increasing number of 'drop-restoration' cycles has no significant impact on the restored reflectance in the visible spectral region, but there is a gradual decline in the ultraviolet. This observation will be discussed later.

The behavior of the Al mirrors is very similar to that observed for Be mirrors [5,6], and further comparison with the behavior of Be mirrors, shown in Fig. 5, is warranted. For mirrors of both mate-

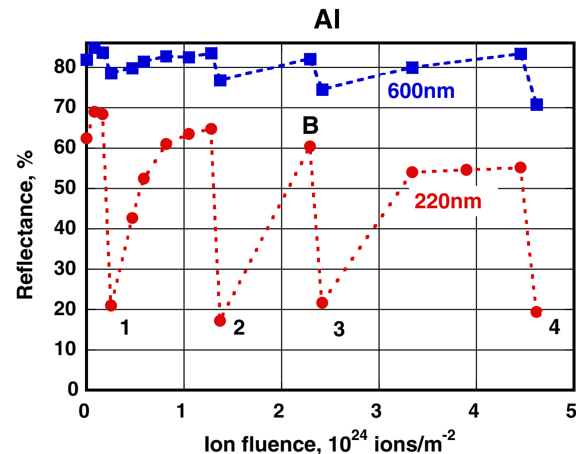

Fig. 4. Dependence of reflectance on total ion fluence at two wavelengths for Al sample. The sharp drops are the result of bombardment with 1350 eV energy ions (stages 1, 2 and 4) and with wide (100–1500 eV) energy-distributed ions (stage 3).

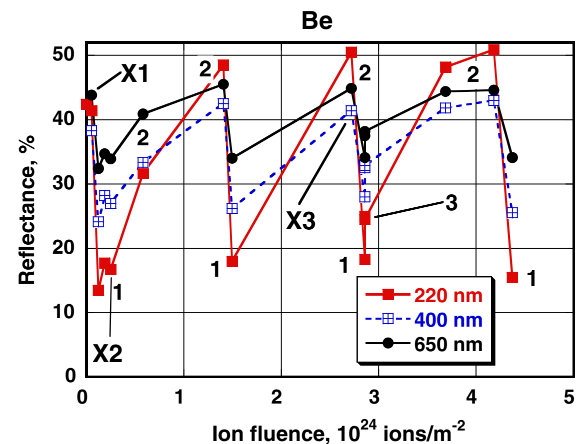

Fig. 5. Dependence of reflectance at indicated wavelengths for Be mirror sample on total ion fluence. (1) Drop of reflectance due to bombardment with ions 1350 eV, (2) restoration of reflectance due to bombardment with ions 60 eV and (3) vacuum annealing after the drop of reflectance. Points marked as X1, X2, X3 correspond to ion fluences when XPS measurements were done (Fig. 6).

rials, short exposures (~10^{23} ions/m^2) to keV-range D^+ ions results in a significant decrease in the reflectance, while much longer exposure to low-energy ions contributed to a restoration of the reflectance. Vacuum annealing was not found to be effective at restoring the reflectance of Be mirrors (Fig. 5), and thus was not part of the present Al-mirror program.

Sputter–XPS analysis was performed on both Al and Be mirrors following both high-energy and low-energy ion bombardment. For the Be mirror, analysis points are indicated on Fig. 5 by X1, X2 and X3. The ratio between BeO and Be was estimated as a function of sputtering time, Fig. 6a. Comparing the results at X1 (♦) and X2 (●), it is clear that exposure to keV ions has resulted in an oxide layer several-times thicker than the original. Long-term exposure to low-energy ions (X3, ■) has the opposite effect of restoring the oxide layer to its original thickness. Similar measurements were made on two specially-prepared Al specimens (which were not polished to a mirror finish), with similar qualitative results, Fig. 6b; the oxide-containing layer is thicker after exposure to keV ions and decreases following the much longer exposure to low-energy ions.

Results from sputter Auger analysis are presented in Fig. 7, and show a qualitative agreement with the XPS results. For the initial surface, the dependence of Al, O and AlO as a function of sputtering time indicate that there is no clear border between the surface layer and the substrate. This may be due in part to the polishing

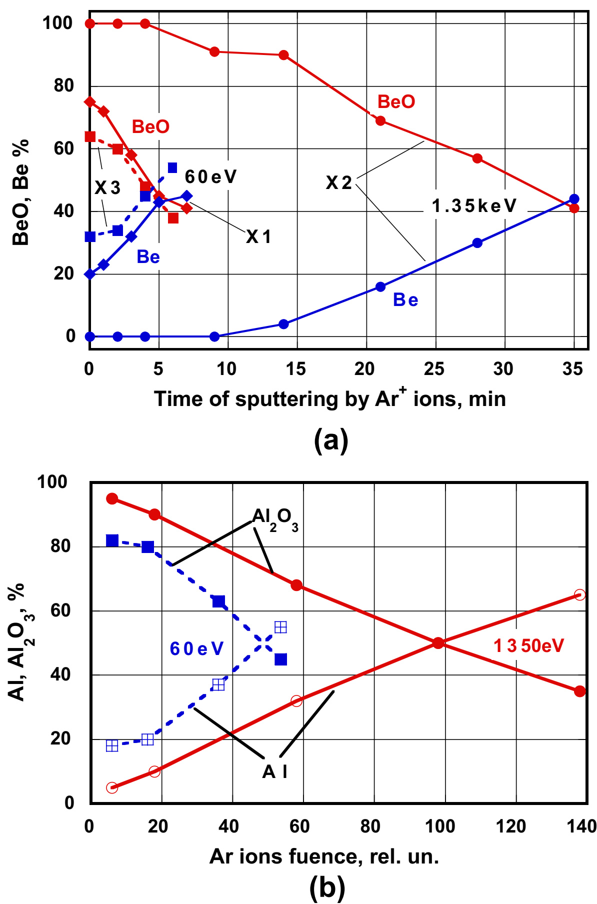

Fig. 6. (a) XPS data for Be mirror sample exposed to deuterium plasma ions: ♦ – Ar ion cleaning (X1 in Fig. 5), E_i = 300 eV; ● – decrease of reflectance due to D^+ ion bombardment, E_i = 1350 eV (X2 in Fig. 5); ■ – restoration of reflectance due to exposure to D^+ ions, E_i = 60 eV after the second drop of reflectance (X3 in Fig. 5). (b) XPS data for Al mirror samples exposed to deuterium plasma ions with low and high ion energy.

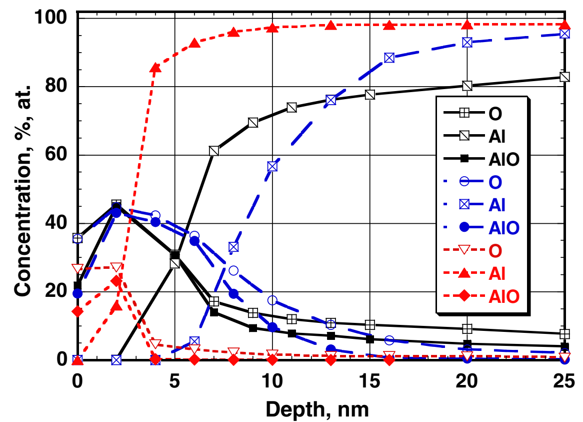

Fig. 7. Data of Auger. Points and solid lines – initial; points connected with broken lines – after bombardment with 1350 eV ions; points connected with dotted lines – long-time exposure to ions with 60 eV following bombardment with 1350 eV ions.

procedure, given the softness of the Al alloy. After exposure to 1.35 keV ions, the border between the surface layer and the substrate becomes sharper. If we use the position of the half-amplitude of the Al signal as an indication of the film thickness, the surface layer has become noticeably thicker following the keV-bombardment. More importantly, however, is the clear evidence that the surface layer has become much thinner following long exposure to low-energy ions (the surface layer/substrate boundary in Fig. 7 is now seen at the depth ~3 nm).

In our analysis of the SIMS mass-spectra, we divided the observed species into two general groups. In the first group we include the positive (and negative) ions of Al, O, and fragments of aluminum oxide, in particular, AlO (the mass 102 corresponding to aluminum oxide, Al_2O_3, was out of the limit of mass measurements). In Fig. 8a are shown the depth profiles of secondary ions O^+ for the three exposure conditions. As seen, in the immediate proximity to the surface, the ion currents are much higher and the peak width is significantly narrower for the long-time cleaned sample in comparison with the initial sample and the one exposed to 1.35 keV ions. This suggests that the near-surface layer of the long-time cleaned sample consists mainly of aluminum oxide. The shape of the depth profile curves for $^{16}O^+$, $^{16}O^-$, $^{43}AlO^-$, $^{43}AlO^+$ and $^{27}Al^+$ ions correlates quite well with data of Auger spectroscopy shown in Fig. 7. The thickness of the oxidized layer estimated from these curves depends on the experimental procedure: it is 8–10 nm for a sample that was cleaned only, ~15 nm after the sample was exposed to impact of 1.35 keV ions (drop of reflectance), and not more than 5 nm after following long term exposure to low-energy ions, 60 eV, (restoration of reflectance). It is worthy of note that there is a quite good agreement of these data for the 'dropped sample' and 'restored sample' with those obtained with ellipsometry (Tables 1 and 2).

The second group consists of molecules and fragments that contain deuterium. Unfortunately, of the possible compounds of Al and D discussed in [8] we did not have the ability to identify clearly either $Al(OD)_3$ or its fragment $Al(OD)_2$ whose masses coincide with that of the Al_3^+ cluster and with the ^{63}Cu isotope, respectively. However, the signal at mass 45 is identified as the $AlOD^+$ fragment. The graphs of Figs. 8b and c show that higher compositions of the D^- and hydroxide fragment ions are found in the sample bombarded with keV-energy ions, and much lower concentrations found in the sample which has been exposed to all three procedures: short cleaning, bombardment with 1.35 keV ions, and long term exposure to low-energy ions.

The surface analysis results allow us to gain an understanding of the processes involved during the ion bombardment of Al and

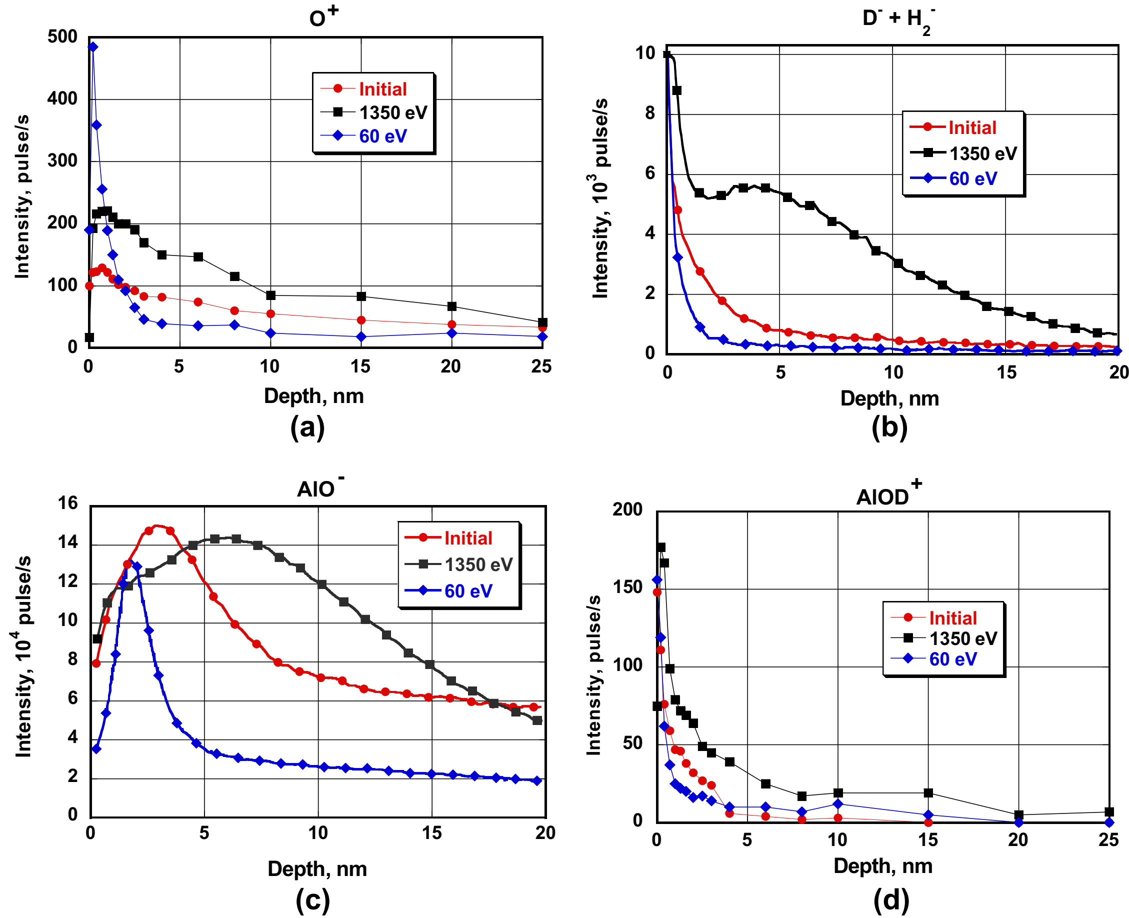

Fig. 8. Data of SIMS analysis of the composition of the near-surface layer for ions: O^+ (a), H_2^-+D^- (b), AlO^-, and for $AlOD^+$. The depth profiles of the yields of secondary ions ejected from the surface of aluminum samples exposed: for only short time to low-energy ions ('initial', circles), after following bombardment with 1.35 keV ions ('1350 eV', squares), after long-time exposure to low-energy ions ('60 eV', diamonds).

Table 2
Parameters of surface film at the end of the cycle 2 (Fig. 4) within BEMA model.

n_f	k_f	d_f (nm)	R (%)	f_{Al}	$f_{Al_2O_3}$	f_{voids}	σ
1.88	3.9	4	81	0.65	0.22	0.13	0.10

Be mirrors. A short bombardment by keV-range D^+ ions, under the experimental conditions of the DSM-2 facility, which includes small amounts of water vapor in the residual gas, results in an increase in thickness of the oxidized surface layer. In particular, the formation of Al or Be hydroxides is postulated since, in the case of Be, BeO films do not have a large impact on reflectance (the extinction coefficient of BeO is close to zero [15]). A subsequent exposure to low-energy ions leads to a gradual reduction of the oxide layer thickness, and specifically to a breakdown of the hydroxides.

4. Application of ellipsometry data for substantiation of mathematic models for analysis of the composition and structure of the surface

Ellipsometry is a very sensitive method for the study of oxidizing processes on metallic surfaces; however, an accurate model of the surface structure is required in order to obtain a correct interpretation of an experiment. The results presented above give us good reasons for selecting specific models, and below we describe models with increasing complexity used to model the current system.

1. We begin with a bare surface model with an unknown index of refraction, N_0. This simple model results were not in good agreement with the experimental data for our case.
2. To refine the model, we can assume a bare surface, but microscopically rough. This leads to what is known as the effective medium model, with a surface layer consisting of voids (absence of material) and aluminum metal. Using the Bruggeman effective medium approximation (BEMA model (2)) the effective complex refractive index N_0 of the effective medium can be found from (e.g., [14]):

$$f_{Al}\frac{N_{Al}^2 - N_0^2}{N_{Al}^2 + 2N_0^2} + f_v\frac{1 - N_0^2}{1 + 2N_0^2} = 0, \quad f_{Al} + f_v = 1, \tag{4}$$

where f_{Al} is the volume fraction of Al metal in the voids-Al mixture, f_v is the fraction of voids and N_{Al} is the refractive index of Al, which was obtained either from the literature [1] or from apparent values of N_0 for the initial specimen (the best reflecting one). An isotropic mixture of Al and voids was assumed. This model also was not good enough.
3. The above model was extended to include a mixture of voids, Al, and Al_2O_3 [$Al(OH)_3$, AlOOH]. The BEMA can then be used to compute the effective index N_0 from the constituents:

$$f_{Al}\frac{N_{Al}^2 - N_0^2}{N_{Al}^2 + 2N_0^2} + f_{Al_2O_3}\frac{N_{Al_2O_3}^2 - N_0^2}{N_{Al_2O_3}^2 + 2N_0^2} + f_v\frac{1 - N_0^2}{1 + 2N_0^2} = 0. \tag{5}$$

Here $f_{Al}, f_{Al_2O_3}, f_v$ are the volume fractions of Al, Al_2O_3 and voids, respectively; $f_{Al} + f_{Al_2O_3} + f_v = 1$.

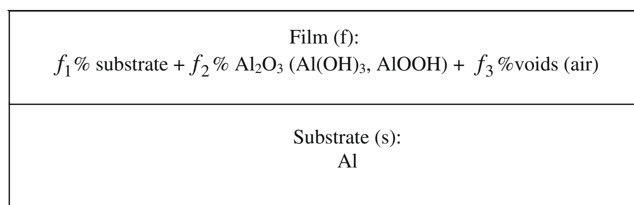

Fig. 9. The structure of the surface of the Al mirror sample in the BEMA model at the stage 3 (Table 1).

The measured experimentally ellipsometry parameters contain information on reflected light: Ψ – about intensity and is not influenced by the appearance of thin transparent deposits, and Δ – about the phase (Eq. (1)). The increase in thickness of a dielectric film results primarily in the phase change, while the appearance of a thin metallic film results in a change of intensity. Therefore, one can expect that the increase in thickness of a complex film containing a metal component would result in changes to both ellipsometry parameters, as observed in our experimental data (Fig. 2). Thus, the present experimental data along with some published results served as the basis for modeling of inhomogeneous layers Al–O in the BEMA model, which is schematically shown in Fig. 9.

The specimen was modeled as an infinite rough layer on an Al substrate, with the roughness consisting of mixture of oxide (Al_2O_3, $Al(OH)_3$, AlOOH), substrate material (Al) and voids filled with air. Table 2 contains the model parameters which provide the best fit to the experiment. It should be emphasized that $n_s < n_f > n_{air}$ but following the chemical reactions associated with the low-energy ion bombardment $n_f \rightarrow n_s$, i.e., decreases. This results in an increase of the reflectivity as observed. We can see that the alignment of volume fractions of Al (f_{Al}), Al_2O_3 ($f_{Al_2O_3}$) and voids (f_{voids}) and the film thickness after reflectance restoration (d_f = 4 nm in Table 2) correlates quite well with the data of sputter Auger analysis and SIMS (≈3 nm in Figs. 7 and 8). That means that increasing of 'drop-restoration' cycle number leads to the increase of roughness (appearance of voids) and thickness of a complex film on the mirror surface (Table 2). We can see (Table 1) that the thickness of the film grows already at the end of the second stage. The fact that the fitting quality σ (Eq. (3)) (Table 2, last column) is much larger means that we have to use more complex real model of the surface already at the end of the second 'drop-restoration' cycle (probably double-layer model). It also means that the reflectivity R should decrease along with increase of 'drop-rise' cycle number and just this is obtained experimentally (Fig. 4). But we have no reason for principal alteration in the model within the framework of the present investigation.

5. Discussion

The fact that the first 'drop-restoration' cycle resulted in almost full restoration of Al mirror reflectance (Fig. 4) indicates that irreversible changes to the mirror surface were not responsible for the decrease in reflectance. With subsequent 'drop-restoration' cycles, however, a gradual decrease in the restored reflectance is observed. The ellipsometry parameter Δ defines the phase shift between p- and s-components of light reflected from a mirror specimen, and its recovery following low-energy ion bombardment (Fig. 2) is a clear indication that the 'drop-restoration' procedure is not related to changes in material stoichiometry or the development of surface defects. We are thus led to the conclusion that the drop in reflectance due to keV ions is due to some chemical process on the mirror surface. As in Refs. [5,6] this chemical process is thought to involve the oxide film which exists on all Al surfaces, with an initial thickness of a few nm [7]. To help in our understanding, we briefly compare the current experimental conditions with other experiments where modification of the chemical composition of an Al-oxide layer was observed.

During the discharge on, with deuterium as the working gas, using a mass spectrometer we observe primary mass peaks (masses 1–4) associated with H and D, but also smaller peaks at mass 17–20. Assuming that these small peaks at least partly correspond to either water or OH radicals, an obvious source of oxygen is available in the system. Thus the possibility exists for the full or partial transformation of Al_2O_3 into hydroxide $Al(OD)_3$ or into intermediate compounds such as AlOOD, as was observed in Refs. [8–10].

Besides the transformation of Al_2O_3 into hydroxide, an increase in thickness of the oxygen-containing surface layer is possible when oxygen-containing ions are incident on a surface together with deuterium ions. A similar process was observed in Refs. [16,17] during the exposure of beryllium to deuterium ions or atoms. Based on SIMS analysis, the authors of [17] concluded that the increase in the thickness of the oxygen-containing surface layer was largely due to the formation of beryllium hydroxide, $Be(OD)_2$. Given the diagonal analogy between Be and Al [7], similar processes might be expected for Al, i.e., appearance and growth of an oxygen-containing film partly composed of hydroxide $Al(OD)_3$ and compound AlOOD.

Consistent with this process is the observed decrease in the refraction coefficient n_f with increasing ion fluence (Table 1). This follows from a comparison of the densities for Al_2O_3 (3.97 g/cm^3), AlOOH (3.01 g/cm^3) and $Al(OH)_3$ (2.42 g/cm^3) [9], and the general trend of a decrease in n_f at lower densities.

The recovery of reflectance following the subsequent long-term bombardment with low-energy (~50 eV) deuterium ions is somehow connected with the removal of the oxide–hydroxide layer. In both the current experiments, and previous ones with Be [5,6], a low-energy ion fluence of ~10–20 times that of the keV ion fluence was required to complete the restoration. The fact that the complete restoration of reflectance does not occur after several 'drop-restoration' cycles (Fig. 4) is attributed to the gradual development of small-scale surface relief (roughness) as a result of keV ion sputtering, with a corresponding decrease of the specular component of the reflected light. This is consistent with the findings for Be mirrors [5], and is directly observed for the present specimens by scanning electron microscopy, Fig. 10.

We propose the following mechanism to explain the different processes on Be and Al mirror samples exposed to keV and low-energy ions of deuterium plasma in conditions of the experimental stand DSM-2. For keV-energy ions the partial transformation of oxide into hydroxides takes place and in addition, the thickness of oxidized layer increases with ion fluence. When afterwards the samples is exposed to low-energy ions (~50 eV) the chemical sputtering of the film containing the mixture of oxides and hydroxides (Al_2O_3, $Al(OD)_3$ and AlOOD in the case of Al mirror) prevails over oxide-hydroxide transformation, thus leading to decrease of the thickness of oxidized layer and to gradual restoration of optical properties.

When discussing the relation of these results to first mirrors in ITER, it should be noted that the described process results in the oxygen enrichment of the film as compared to aluminum oxide (O/Al = 3:1 for $Al(OD)_3$ and O/Al = 2:1 for Al(OOD), whereas O/Al = 1.5:1 for Al_2O_3), therefore it is possible only when oxygen-containing molecules (or their radicals) are present in the plasma close to the mirror surface. In the absence of oxygen, bombardment of mirror surface with atoms and ions of hydrogen isotopes will lead to transformation of oxide into hydroxide without noticeable rise of the film thickness, i.e., without strong effect on the reflectance, as the natural oxide layer thickness is small. Thus the behavior in ITER of Al mirrors or mirrors with Al_2O_3 coating (as suggested in

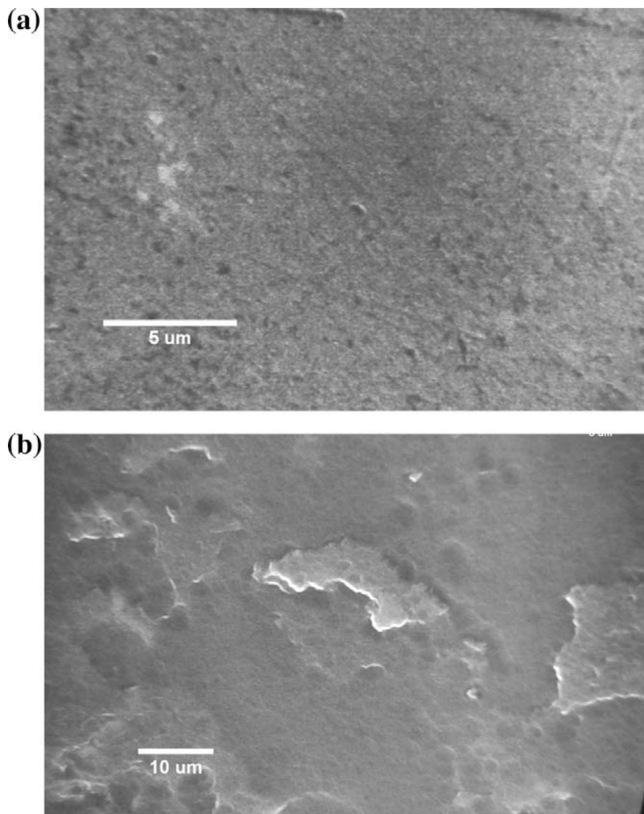

Fig. 10. SEM photos of the surface of Al mirror sample initial (a) and after (b) the last exposure to ions of deuterium plasma (Fig. 4).

[18]) would depend on the working conditions: energy and fluxes to mirror surface of ions and atoms of hydrogen isotopes, fluxes of oxygen-containing molecules, mirror temperature, etc. This statement would also be valid for mirrors that have other dielectric coatings of a high reactive ability to form hydrides.

6. Conclusion

We have studied the effects of the ion-induced modification of aluminum alloy mirrors, under bombardment by deuterium plasma ions. The following general conclusions may be made:

1. A decrease in reflectance is observed in the $\lambda = 220–750$ nm range when Al mirrors are exposed to keV-energy range ions from a deuterium plasma, but a restoration of the reflectance takes place when the mirror is subsequently exposed to low-energy ions ($\sim$50 eV), again from a deuterium plasma. Thus, it was shown that the diagonal analogy between Be and Al becomes apparent not only for their chemical properties but for optical characteristics also.
2. As indicated by various surface analyses techniques, the reversible changes in reflectance are due to an ion-induced transformation of the surface oxide layer. The higher energy bombardment in the presence of oxygen leads to the creation of a thicker surface layer with a large hydroxide content, while the lower energy bombardment leads to the gradual reduction of the thickness of the modified surface layer.
3. The microscopic surface roughness (detected by ellipsometry) can be best described by a model which assumes a combination of Al plus Al_2O_3 ($Al(OD)_3$ and AlOOD) plus voids in fractions determined by the Bruggeman effective medium approximation. After long-term ion bombardment of the Al alloy mirror, the effective medium calculations indicate that effects due to oxides are minimal (the fraction of oxide was estimated to be about 0.22).
4. The surface-modification processes described above can limit the use of Al mirrors to those locations in ITER where they will not be exposed to energetic hydrogen isotopes and oxygen-containing molecules or ions.
5. Optical ellipsometry is a very effective method for studying microscopic changes on mirror surfaces taking place under bombardment with ions of different energy at the early stage of the surface structure development. However, it is clear that more complicated ellipsometric models must be used in the analysis of Al mirrors exposed to ITER-like conditions, typical of high vacuum devices (i.e., with some amount of water vapor).

References

[1] E.D. Palik (Ed.), Handbook of Optical Constants of Solids, Academic Press, San Diego, California, 1985.
[2] V.S. Voitsenya, A.F. Bardamid, Yu.N. Borisenko, et al., Plasma Dev. Oper. 7 (1999) 243.
[3] V.S. Voitsenya, V.G. Konovalov, A.F. Shtan‘, et al., Rev. Sci. Instrum. 70 (1) (1999) 790.
[4] Y. Yamamura, H. Tawara, ADNDT 62 (1996) 149.
[5] A.F. Bardamid, A.I. Belyayeva, V.N. Bondarenko, et al., J. Nucl. Mater. 313–316 (2003) 112.
[6] V.S. Voitsenya, A.F. Bardamid, V.N. Bondarenko, et al., J. Nucl. Mater. 329–333 (2004) 1476.
[7] Martin Silberberg, Chemistry: The Molecular Nature of Matter and Change, McGraw-Hill, 2004 (1216p, Chapter 14.5 Group 3A(13): The Boron Family).
[8] T. Hernandez, A. Moronõ, E.R. Hodgson, Fusion Eng. Des. 69 (2003) 177.
[9] J.M. Schneider, A. Anders, B. Hjörvarsson, et al., Appl. Phys. Lett. 74 (1999) 200.
[10] J.M. Schneider, K. Larsson, Lu Jun, et al., Appl. Phys. Lett. 80 (2002) 1144.
[11] A.F. Bardamid, V.T. Gritsyna, V.G. Konovalov, et al., Surf. Coat. Technol. 103–104 (1998) 365.
[12] D.V. Orlinski, V.S. Voitsenya, K.Yu. Vukolov, Plasma Dev. Oper. 15 (2007) 33.
[13] S. Tolansky, High Resolution Spectroscopy, New York, Chicago, 1947.
[14] H.G. Tompkins, W.A. McGahan, Spectroscopic Ellipsometry and Reflectometry: A User's Guide, John Wiley and Sons, New York, 1999.
[15] D.F. Edwards, R.H. White, Beryllium oxide, in: E.D. Palik (Ed.), Handbook of Optical Constants of Solids, Academic Press, San Diego, California, 1991. p. 805.
[16] R.A. Langley, J. Nucl. Mater. 85–87 (1979) 1123.
[17] V.M. Sharapov, V.Kh. Alimov, L.E. Gavrilov, J. Nucl. Mater. 258–263 (1998) 803.
[18] E.E. Mukhin, G.T. Razdobarin, V.V. Semenov, et al., Prospects of use of diagnostic mirrors with transparent protection layer in burning plasma experiments, in: F.P. Orsitto, et al. (Eds.), AIP Conference Proceedings, vol. 988, Burning Plasma Diagnostics, Melville, New York, 2008, pp. 365–369.